
































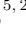


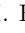







Discovery of a Gamma-ray Black Widow Pulsar by GPU-accelerated Einstein@Home Supplementary Material

L. NIEDER ^{1,2} C. J. CLARK ³ D. KANDEL ⁴ R. W. ROMANI ⁴ C. G. BASSA ⁵ B. ALLEN ^{1,6,2} A. ASHOK ^{1,2}
I. COGNARD ^{7,8} H. FEHRMANN ^{1,2} P. FREIRE ⁹ R. KARUPPUSAMY ⁹ M. KRAMER ^{9,3} D. LI ^{10,11}
B. MACHENSCHALK ^{1,2} Z. PAN ¹⁰ M. A. PAPA ^{1,6,2} S. M. RANSOM ¹² P. S. RAY ¹³ J. ROY ¹⁴ P. WANG ¹⁰
J. WU ⁹ C. AULBERT ^{1,2} E. D. BARR ⁹ B. BEHESHTIPOUR ^{1,2} O. BEHNKE ^{1,2} B. BHATTACHARYYA ¹⁴
R. P. BRETON ³ F. CAMILO ¹⁵ C. CHOQUET ¹⁶ V. S. DHILLON ^{17,18} E. C. FERRARA ^{19,20} L. GUILLEMOT ^{7,8}
J. W. T. HESSELS ^{5,21} M. KERR ¹³ S. A. KWANG ²² T. R. MARSH ²³ M. B. MICKALIGER ³ Z. PLEUNIS ^{24,25}
H. J. PLETSCH ¹ M. S. E. ROBERTS ^{26,27} S. SANPA-ARSA ²⁸ AND B. STELTNER ^{1,2}

¹Max-Planck-Institut für Gravitationsphysik (Albert-Einstein-Institut), 30167 Hannover, Germany

²Leibniz Universität Hannover, 30167 Hannover, Germany

³Jodrell Bank Centre for Astrophysics, Department of Physics and Astronomy, The University of Manchester, M13 9PL, UK

⁴KIPAC/Dept. of Physics, Stanford University, Stanford, CA 94305, USA

⁵ASTRON, The Netherlands Institute for Radio Astronomy, Oude Hoogeveensedijk 4, 7991 PD Dwingeloo, The Netherlands

⁶Department of Physics, University of Wisconsin–Milwaukee, P.O. Box 413, Milwaukee, WI 53201, USA

⁷Laboratoire de Physique et Chimie de l’Environnement et de l’Espace, Université d’Orléans / CNRS, F-45071 Orléans Cedex 02, France

⁸Station de radioastronomie de Nançay, Observatoire de Paris, CNRS/INSU, F-18330 Nançay, France

⁹Max-Planck-Institut für Radioastronomie, auf dem Hügel 69, 53121 Bonn, Germany

¹⁰National Astronomical Observatories, Chinese Academy of Sciences, Beijing 100101, China

¹¹NAOC-UKZN Computational Astrophysics Centre, University of KwaZulu-Natal, Durban 4000, South Africa

¹²National Radio Astronomy Observatory, 520 Edgemont Rd., Charlottesville, VA USA 22903

¹³Space Science Division, Naval Research Laboratory, Washington, DC 20375-5352, USA

¹⁴National Centre for Radio Astrophysics, Tata Institute of Fundamental Research, Pune 411 007, India

¹⁵South African Radio Astronomy Observatory, 2 Fir Street, Black River Park, Observatory 7925, South Africa

¹⁶Résidence Le Dauphiné, rue Jean Bleuzen, Vanves, France

¹⁷Department of Physics and Astronomy, University of Sheffield, Sheffield S3 7RH, UK

¹⁸Instituto de Astrofísica de Canarias, E-38205 La Laguna, Tenerife, Spain

¹⁹NASA Goddard Space Flight Center, Greenbelt, MD 20771, USA

²⁰Department of Astronomy, University of Maryland, College Park, MD 20742, USA

²¹Anton Pannekoek Institute for Astronomy, University of Amsterdam, Science Park 904, 1098 XH Amsterdam, The Netherlands

²²Department of Physics, University of Wisconsin–Milwaukee, P.O. Box 413, Milwaukee, WI 53201, USA

²³Astronomy and Astrophysics Group, Department of Physics, University of Warwick, Coventry CV4 7AL, UK

²⁴Department of Physics, McGill University, 3600 rue University, Montréal, QC H3A 2T8, Canada

²⁵McGill Space Institute, McGill University, 3550 rue University, Montréal, QC H3A 2A7, Canada

²⁶New York University Abu Dhabi, P.O. Box 129188, Abu Dhabi, UAE

²⁷Eureka Scientific, Inc. 2452 Delmer Street, Suite 100, Oakland, CA 94602-3017, USA

²⁸National Astronomical Research Institute of Thailand (Public Organization), 260 Moo 4, T. Donkaew, A. Maerim, Chiang Mai, 50180, Thailand

(Received 2020 September 1; Revised 2020 September 22; Accepted 2020 September 25; Published 2020 October 22)

CONTINUOUS GRAVITATIONAL WAVES

Acknowledging the possibility of mismatches between the pulsar rotation frequency and the gravitational-wave frequency, we perform an \mathcal{F} -statistic search in

a ~ 2 Hz band around twice the rotation frequency, a factor of 10^{-3} of the gravitational-wave frequency, similarly to what was done in [Abbott et al. \(2019\)](#) and also extend the spin-down search to the range $2\dot{f} \in (-1.260, -1.2216) \times 10^{-15}$ Hz s⁻¹. Overall, we use 2.4×10^9 templates resulting in an average mismatch of 1%. We examine the results in 10 mHz-wide bands. The most significant $2\mathcal{F}$ values from each band are consistent with the noise-only expectation, apart from six

outliers that can be ascribed to a disturbance in L1 around ≈ 1016.32 Hz. We set upper limits in each band. The values are plotted in Figure 1. The mean value is 1.3×10^{-25} and it is higher than the targeted search upper limit, consistently with the larger volume of searched wave shapes.

Table 1. Upper limits on $h_0^{95\%}$ in each of the 10 mHz bands.

Start freq. (Hz)	$h_0^{95\%} \times 10^{-25}$
1015.408	$1.34^{+0.25}_{-0.23}$
1015.418	$1.23^{+0.22}_{-0.23}$
1015.428	$1.36^{+0.27}_{-0.26}$
1015.438	$1.3^{+0.26}_{-0.24}$
1015.448	$1.3^{+0.24}_{-0.24}$
1015.458	$1.33^{+0.25}_{-0.23}$
1015.468	$1.26^{+0.24}_{-0.23}$
1015.478	$1.42^{+0.27}_{-0.25}$
1015.488	$1.4^{+0.26}_{-0.25}$
1015.498	$1.35^{+0.26}_{-0.25}$
1015.508	$1.31^{+0.25}_{-0.23}$
1015.518	$1.34^{+0.28}_{-0.27}$
1015.528	$1.48^{+0.29}_{-0.28}$
1015.538	$1.35^{+0.27}_{-0.25}$
1015.548	$1.22^{+0.21}_{-0.22}$
1015.558	$1.41^{+0.28}_{-0.26}$
1015.568	$1.36^{+0.26}_{-0.24}$
1015.578	$1.28^{+0.26}_{-0.25}$
1015.588	$1.26^{+0.23}_{-0.22}$
1015.598	$1.35^{+0.26}_{-0.24}$
1015.608	$1.29^{+0.24}_{-0.24}$
1015.618	$1.35^{+0.26}_{-0.24}$
1015.628	$1.35^{+0.29}_{-0.28}$
1015.638	$1.28^{+0.24}_{-0.22}$
1015.648	$1.25^{+0.23}_{-0.22}$
1015.658	$1.26^{+0.24}_{-0.23}$
1015.668	$1.25^{+0.22}_{-0.23}$
1015.678	$1.23^{+0.23}_{-0.23}$
1015.688	$1.2^{+0.21}_{-0.22}$
1015.698	$1.3^{+0.25}_{-0.23}$
1015.708	$1.32^{+0.26}_{-0.24}$
1015.718	$1.23^{+0.28}_{-0.3}$
1015.728	$1.3^{+0.25}_{-0.23}$
1015.738	$1.26^{+0.23}_{-0.22}$

Table 1 *continued*

Table 1 (*continued*)

Start freq. (Hz)	$h_0^{95\%} \times 10^{-25}$
1015.748	$1.4^{+0.26}_{-0.25}$
1015.758	$1.23^{+0.22}_{-0.23}$
1015.768	$1.41^{+0.26}_{-0.24}$
1015.778	$1.27^{+0.31}_{-0.33}$
1015.788	$1.34^{+0.26}_{-0.24}$
1015.798	$1.22^{+0.29}_{-0.32}$
1015.808	$1.21^{+0.21}_{-0.22}$
1015.818	$1.23^{+0.21}_{-0.21}$
1015.828	$1.32^{+0.25}_{-0.24}$
1015.838	$1.23^{+0.21}_{-0.21}$
1015.848	$1.21^{+0.22}_{-0.23}$
1015.858	$1.47^{+0.29}_{-0.27}$
1015.868	$1.29^{+0.25}_{-0.23}$
1015.878	$1.28^{+0.24}_{-0.23}$
1015.888	$1.29^{+0.25}_{-0.24}$
1015.898	$1.32^{+0.24}_{-0.24}$
1015.908	$1.27^{+0.23}_{-0.22}$
1015.918	$1.29^{+0.24}_{-0.24}$
1015.928	$1.44^{+0.29}_{-0.27}$
1015.938	$1.2^{+0.21}_{-0.22}$
1015.948	$1.24^{+0.22}_{-0.22}$
1015.958	$1.27^{+0.23}_{-0.22}$
1015.968	$1.26^{+0.23}_{-0.23}$
1015.978	$1.2^{+0.21}_{-0.23}$
1015.988	$1.38^{+0.27}_{-0.25}$
1015.998	$1.29^{+0.26}_{-0.24}$
1016.008	$1.27^{+0.24}_{-0.23}$
1016.018	$1.27^{+0.24}_{-0.23}$
1016.028	$1.37^{+0.27}_{-0.25}$
1016.038	$1.24^{+0.21}_{-0.21}$
1016.048	$1.24^{+0.23}_{-0.23}$
1016.058	$1.32^{+0.26}_{-0.25}$
1016.068	$1.4^{+0.26}_{-0.25}$
1016.078	$1.39^{+0.28}_{-0.26}$
1016.088	$1.33^{+0.26}_{-0.25}$
1016.098	$1.4^{+0.27}_{-0.26}$
1016.108	$1.26^{+0.23}_{-0.23}$
1016.118	$1.31^{+0.25}_{-0.24}$
1016.128	$1.35^{+0.26}_{-0.24}$
1016.138	$1.28^{+0.25}_{-0.23}$
1016.148	$1.2^{+0.21}_{-0.22}$

Table 1 *continued*

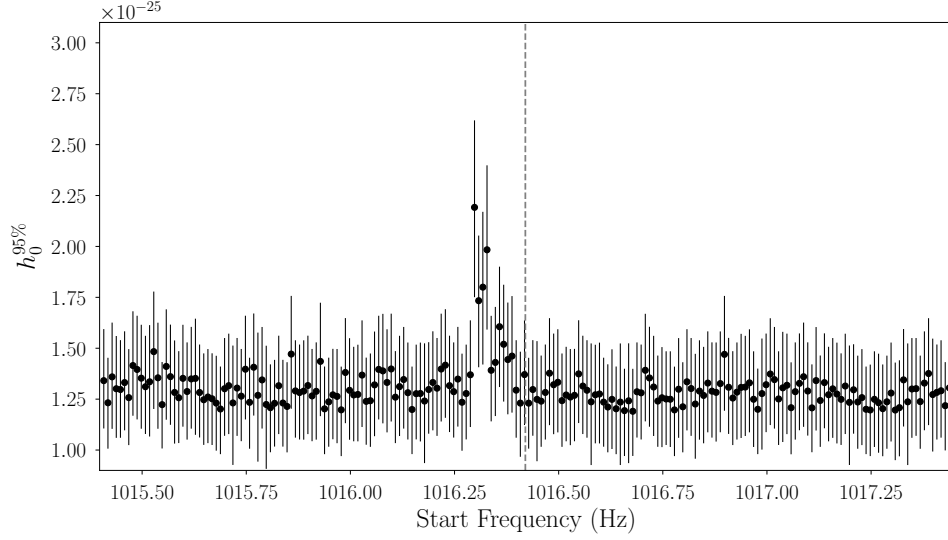


Figure 1. 95% confidence upper limits on the gravitational-wave amplitude in 10 mHz bands around twice the rotation frequency of PSR J1653–0158, which is indicated by the gray dashed line. The bars indicate a conservative estimate of the uncertainty on the upper limit values. The “spike” does not indicate a detection: it is due to a disturbance in L1 around ≈ 1016.32 Hz.

Table 1 (*continued*)

Start freq. (Hz)	$h_0^{95\%} \times 10^{-25}$
1016.158	$1.28^{+0.24}_{-0.22}$
1016.168	$1.28^{+0.25}_{-0.24}$
1016.178	$1.24^{+0.28}_{-0.3}$
1016.188	$1.3^{+0.23}_{-0.22}$
1016.198	$1.33^{+0.25}_{-0.23}$
1016.208	$1.3^{+0.25}_{-0.23}$
1016.218	$1.4^{+0.27}_{-0.26}$
1016.228	$1.42^{+0.27}_{-0.26}$
1016.238	$1.32^{+0.25}_{-0.23}$
1016.248	$1.29^{+0.24}_{-0.23}$
1016.258	$1.35^{+0.26}_{-0.23}$
1016.268	$1.23^{+0.24}_{-0.24}$
1016.278	$1.28^{+0.24}_{-0.23}$
1016.288	$1.37^{+0.27}_{-0.26}$
1016.298	$2.19^{+0.43}_{-0.44}$
1016.308	$1.73^{+0.32}_{-0.33}$
1016.318	$1.8^{+0.37}_{-0.38}$
1016.328	$1.98^{+0.41}_{-0.39}$
1016.338	$1.39^{+0.27}_{-0.25}$
1016.348	$1.43^{+0.27}_{-0.26}$
1016.358	$1.61^{+0.29}_{-0.3}$
1016.368	$1.52^{+0.29}_{-0.28}$
1016.378	$1.44^{+0.28}_{-0.27}$

Table 1 *continued*

Table 1 (*continued*)

Start freq. (Hz)	$h_0^{95\%} \times 10^{-25}$
1016.388	$1.46^{+0.29}_{-0.28}$
1016.398	$1.29^{+0.25}_{-0.23}$
1016.408	$1.23^{+0.25}_{-0.26}$
1016.418	$1.37^{+0.27}_{-0.25}$
1016.428	$1.23^{+0.22}_{-0.22}$
1016.438	$1.3^{+0.24}_{-0.23}$
1016.448	$1.25^{+0.29}_{-0.3}$
1016.458	$1.24^{+0.22}_{-0.22}$
1016.468	$1.28^{+0.24}_{-0.23}$
1016.478	$1.38^{+0.27}_{-0.26}$
1016.488	$1.32^{+0.25}_{-0.24}$
1016.498	$1.33^{+0.26}_{-0.25}$
1016.508	$1.24^{+0.23}_{-0.23}$
1016.518	$1.27^{+0.24}_{-0.23}$
1016.528	$1.26^{+0.24}_{-0.24}$
1016.538	$1.27^{+0.23}_{-0.23}$
1016.548	$1.37^{+0.26}_{-0.24}$
1016.558	$1.31^{+0.25}_{-0.24}$
1016.568	$1.29^{+0.25}_{-0.23}$
1016.578	$1.24^{+0.29}_{-0.31}$
1016.588	$1.27^{+0.25}_{-0.24}$
1016.598	$1.28^{+0.25}_{-0.24}$
1016.608	$1.24^{+0.22}_{-0.22}$

Table 1 *continued*

Table 1 (*continued*)

Start freq. (Hz)	$h_0^{95\%} \times 10^{-25}$
1016.618	$1.21^{+0.21}_{-0.22}$
1016.628	$1.25^{+0.25}_{-0.24}$
1016.638	$1.2^{+0.21}_{-0.22}$
1016.648	$1.24^{+0.29}_{-0.31}$
1016.658	$1.19^{+0.21}_{-0.22}$
1016.668	$1.24^{+0.28}_{-0.31}$
1016.678	$1.19^{+0.21}_{-0.22}$
1016.688	$1.29^{+0.24}_{-0.22}$
1016.698	$1.28^{+0.24}_{-0.23}$
1016.708	$1.39^{+0.28}_{-0.25}$
1016.718	$1.35^{+0.25}_{-0.24}$
1016.728	$1.31^{+0.25}_{-0.24}$
1016.738	$1.24^{+0.22}_{-0.22}$
1016.748	$1.26^{+0.25}_{-0.24}$
1016.758	$1.25^{+0.23}_{-0.23}$
1016.768	$1.25^{+0.24}_{-0.23}$
1016.778	$1.2^{+0.21}_{-0.23}$
1016.788	$1.3^{+0.25}_{-0.24}$
1016.798	$1.21^{+0.22}_{-0.22}$
1016.808	$1.34^{+0.26}_{-0.24}$
1016.818	$1.3^{+0.25}_{-0.23}$
1016.828	$1.23^{+0.25}_{-0.27}$
1016.838	$1.29^{+0.25}_{-0.24}$
1016.848	$1.27^{+0.24}_{-0.24}$
1016.858	$1.33^{+0.25}_{-0.24}$
1016.868	$1.29^{+0.24}_{-0.23}$
1016.878	$1.28^{+0.25}_{-0.24}$
1016.888	$1.33^{+0.26}_{-0.24}$
1016.898	$1.47^{+0.29}_{-0.28}$
1016.908	$1.31^{+0.24}_{-0.23}$
1016.918	$1.26^{+0.23}_{-0.23}$
1016.928	$1.28^{+0.24}_{-0.23}$
1016.938	$1.31^{+0.26}_{-0.25}$
1016.948	$1.31^{+0.25}_{-0.24}$
1016.958	$1.33^{+0.26}_{-0.24}$
1016.968	$1.25^{+0.24}_{-0.23}$
1016.978	$1.2^{+0.2}_{-0.22}$
1016.988	$1.28^{+0.27}_{-0.28}$
1016.998	$1.32^{+0.25}_{-0.23}$
1017.008	$1.37^{+0.27}_{-0.25}$
1017.018	$1.35^{+0.26}_{-0.24}$

Table 1 *continued***Table 1** (*continued*)

Start freq. (Hz)	$h_0^{95\%} \times 10^{-25}$
1017.028	$1.25^{+0.23}_{-0.23}$
1017.038	$1.31^{+0.27}_{-0.27}$
1017.048	$1.32^{+0.25}_{-0.24}$
1017.058	$1.21^{+0.22}_{-0.23}$
1017.068	$1.29^{+0.24}_{-0.24}$
1017.078	$1.33^{+0.25}_{-0.23}$
1017.088	$1.36^{+0.27}_{-0.25}$
1017.098	$1.29^{+0.24}_{-0.22}$
1017.108	$1.21^{+0.21}_{-0.22}$
1017.118	$1.34^{+0.26}_{-0.25}$
1017.128	$1.24^{+0.22}_{-0.23}$
1017.138	$1.33^{+0.24}_{-0.22}$
1017.148	$1.27^{+0.24}_{-0.23}$
1017.158	$1.3^{+0.25}_{-0.24}$
1017.168	$1.27^{+0.25}_{-0.24}$
1017.178	$1.25^{+0.23}_{-0.22}$
1017.188	$1.31^{+0.26}_{-0.24}$
1017.198	$1.23^{+0.28}_{-0.31}$
1017.208	$1.3^{+0.22}_{-0.22}$
1017.218	$1.24^{+0.23}_{-0.23}$
1017.228	$1.26^{+0.24}_{-0.23}$
1017.238	$1.2^{+0.21}_{-0.22}$
1017.248	$1.2^{+0.22}_{-0.23}$
1017.258	$1.25^{+0.24}_{-0.23}$
1017.268	$1.23^{+0.24}_{-0.25}$
1017.278	$1.2^{+0.22}_{-0.23}$
1017.288	$1.24^{+0.23}_{-0.23}$
1017.298	$1.28^{+0.25}_{-0.24}$
1017.308	$1.2^{+0.23}_{-0.25}$
1017.318	$1.21^{+0.23}_{-0.24}$
1017.328	$1.34^{+0.25}_{-0.23}$
1017.338	$1.24^{+0.29}_{-0.31}$
1017.348	$1.3^{+0.25}_{-0.24}$
1017.358	$1.3^{+0.25}_{-0.23}$
1017.368	$1.24^{+0.23}_{-0.23}$
1017.378	$1.33^{+0.25}_{-0.23}$
1017.388	$1.38^{+0.27}_{-0.25}$
1017.398	$1.27^{+0.27}_{-0.28}$
1017.408	$1.28^{+0.24}_{-0.23}$
1017.418	$1.29^{+0.25}_{-0.23}$
1017.428	$1.22^{+0.21}_{-0.22}$
1017.438	$1.31^{+0.26}_{-0.25}$

REFERENCES

Abbott, B. P., Abbott, R., Abbott, T. D., et al. 2019,
PhRvD, 99, 122002, doi: [10.1103/PhysRevD.99.122002](https://doi.org/10.1103/PhysRevD.99.122002)